Ethylene adsorption and decomposition on Si(100) 2*1: a semi-empirical quantum chemical study

Ethylene adsorption and decomposition on Si(100) 2 × 1: a semi-empirical quantum chemical study

Pei-Lin Cao†‡ and Ru-Hong Zhou†‡

† China Centre of Advanced Science and Technology (World Laboratory), PO Box 8730, Beijing 100080, People's Republic of China
‡ Department of Physics, Zhejiang University, Hangzhou 310027, People's Republic of China§

Abstract. The interaction of ethylene with the Si(100) 2×1 surface has been studied by a semi-empirical molecular orbital theory using a four-layer silicon cluster model $Si_{29}H_{24}$–C_2H_4. Ethylene is shown to create a di-σ bond with the surface dimer sites, and to rehybridize to a near sp^3 state. Its initial C–C double bond is reduced to nearly a single bond, while its C–H bonds are almost not weakened. Both the ethylene π donation to the surface and the substrate back-donation to the ethylene π^* orbital result in the equilibrium di-σ bonding geometry. The C_2H_4 decomposition behaviour is somewhat different from that for C_2H_2(ads) on Si(100), and C_2H_4(ads) on transition metals. Ethylene favours C–C bond scission first, and then dehydrogenation. The calculated vibrational properties of the C_2H_4(ads) and C_2H_4-induced species confirm the results of a recent HREELS study.

1. Introduction

The adsorption of small unsaturated hydrocarbons (typically C_2H_2, C_2H_4 etc) on silicon surfaces is of interest at present, since the production of β-SiC thin films may be achieved by the thermal decomposition of these adsorbed species [1–8]. The π-bonding system in these small molecules is the active molecular centre for chemisorption on silicon surfaces [9, 10]. A variety of surface techniques, such as LEED, HREELS [1–4], the kinetic uptake method [5], an isotopic mixing study [6] and semi-empirical quantum theories [7, 8] have been applied to these adsorption systems, including C_2H_2–Si(100) [1, 5], C_2H_4–Si(100) [2, 5, 6], C_2H_2–Si(111) [3, 7, 8] and C_2H_4–Si(111) [4].

These recent studies have offered as much information about the interaction mechanism, such as the di-σ bonding geometry [11] for $C_2H_4(C_2H_2)$ on Si(100) 2×1 [2, 5], the saturation coverage of one $C_2H_4(C_2H_2)$ molecule per Si dimer site [5], and the weakening of the C–C triple (or double) bonds [2, 5, 8], but no information was given about the bond lengths or bond angles, nor about the decomposition paths and activation barriers for C_2H_4 on Si(100). On the other hand, the reaction of C_2H_4 and C_2H_2 with transition-metal surfaces is quite well understood owing to the numerous experimental and theoretical studies [12–19]. Thus a comparable theoretical study for C_2H_4, C_2H_2, etc, on Si(100) and (111) surfaces may be especially valuable. As the *ab initio* methods are difficult to use with systems containing too many electrons, we employ a simple molecular orbital theory to assist our understanding, with modest demands on computer resources. We have studied the C_2H_2–Si(100) system

§ Address to which any correspondence should be sent.

using this fast semi-empirical quantum theory [10]. Here, we report the results on C_2H_4–Si(100).

2. Models and method

In this paper, a four-layer silicon cluster model $Si_{29}H_{24}$–C_2H_4 is adopted to simulate the C_2H_4 adsorption and decomposition on Si(100) 2×1 (figure 1). For this reconstructed surface, we use the 2×1 symmetric-dimer model reported by Roberts and Needs [20]. According to this model, the displacements of the first-layer Si atoms making up each dimer are 0.331 Å in the [$\bar{1}$00] direction (closer to the second layer) and ±0.803 Å in the [0$\bar{1}$1] direction (to form dimers). The second-, third- and fourth-layer Si atoms also have some small displacements with respect to their unreconstructed bulk places. The H atoms in the cluster model are used only to saturate the bulk Si dangling bonds as treated in most of the studies.
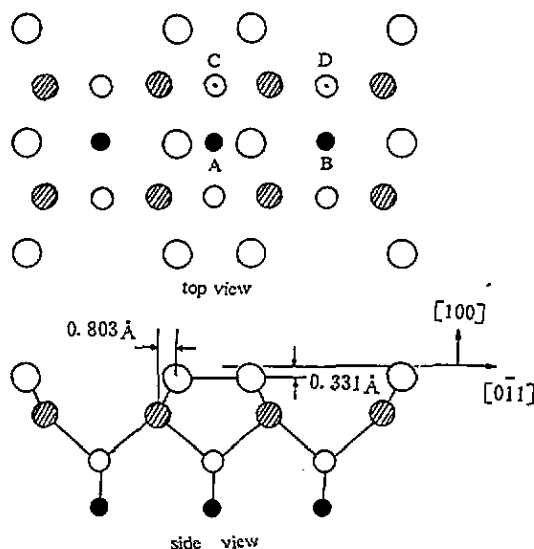

Figure 1. Cluster model $Si_{29}H_{24}$ applied to simulate the Si(100) 2×1 surface: H atoms are used to saturate the bulk dangling bonds and are not plotted for convenience. large open circles, first-layer Si atom; hatched circles, second-layer Si atom; small open circles, third-layer Si atom; full circles, fourth-layer Si atom.

The atom superposition and electron delocalization (ASED) molecular orbital theory is used in the calculation; this theory has been applied successfully to many systems [21–24]. The extended Hückel independent energy represents the binding part of the interaction energy, which is due to electron delocalization, while the atom superposition energy is the sum of repulsive interatomic interactions. This fast method seems appropriate especially for calculating the bond geometries and force constants of complex systems. The atomic parameters used in the calculations are listed in table 1. They are based on the literature ionization potential [25] and Slater orbital exponents [26] with 1.3 eV shifts in the ionization potentials to produce reasonable diatomic SiC charge transfers (increases for Si and decreases for C and H). Using these parameters, the C=C and C–H bond lengths of the free C_2H_4 molecule are overestimated by 0.14 and 0.11 Å, respectively, while the CH stretching, CC stretching and CH_2 scissors frequencies are 3011 cm^{-1}, 1504 cm^{-1} and 1330 cm^{-1}, respectively, in good agreement with the corresponding experimental results of 3019 cm^{-1}, 1623 cm^{-1} and 1342 cm^{-1}.

Table 1. Atomic parameters used in calculations: principal quantum number (n), ionization potential and Slater orbital.

		S			P	
Atom	n	Ionization potential (eV)	ζ (au)	n	Ionization potential (eV)	ζ (au)
Si	3	14.76	1.6344	3	9.45	1.4284
C	2	15.29	1.658	2	9.96	1.618
H	1	12.30	1.20			

3. Results and Discussion

To determine the chemisorption geometry of molecular ethylene, four possible adsorption sites are considered in our calculation, including the bridge site A, the cave site B, the pedestal site C and the valley bridge D (see figure 1). For each adsorption site, we shall calculate the curves of total energy (TE) versus the adsorption height. Here, the adsorption height is defined as the vertical distance of the C=C double bond from the unreconstructed Si(100) surface. By symmetry analysing and former experience [10], we have assumed that the C=C double bond is parallel to the surface. Then the height from the actual surface Si atoms is $h + 0.331$ Å according to the 2×1 symmetric-dimer model [20]. The TE at infinite adsorption height is set at zero.

It is obvious that the TE of the system is related to the adsorption site, the adsorption height, the C–C bond length, the C–H bond length, the CH₂ scissors angle, the CH₂ plane to the surface angle, etc. This means that it is at least a seven-dimensional potential surface, which may be too difficult for us to solve rigorously using the present computer resources. However, fortunately, we can approach the final accurate geometry by some reasonable simplifications and optimization step by step.

Two simple cases are first studied: one is planar C₂H₄ adsorption (sp² hybridization; just free molecule); the other is distorted C₂H₄* adsorption with the angle H–C–H set at 109.47° (sp³ hybridization; the angle of the CH₂ plane to the surface is 54.7°). Figure 2 shows the TE curves versus the adsorption height on the bridge, cave, pedestal and valley bridge sites for these two different structures. It is clear that the planar C₂H₄ is energetically unfavoured, which indicates that the C₂H₄(ads) must be rehybridized. On the other hand the distorted C₂H₄* can adsorb onto the bridge site (the dimer site) to form a di-σ-bonding geometry, but this distorted C₂H₄* structure is also impossible to adsorb onto the pedestal and valley bridge sites as shown in figure 2(b). For the cave site, although a TE minimum appears, this energy is still much higher than zero. Thus, C₂H₄* may also not adsorb onto the cave site. (The further calculation given later confirms this.) As we know, Yoshinobu *et al* [2] suggested that the dimer site is favoured over the cave site because the symmetric SiC stretching vibration (670 cm⁻¹) is excited predominantly by the dipole mechanism, which allows us to deduce that the SiC bond axes are nearly normal to Si(100). However, these workers also pointed out that they could not exclude the possibility that the selection rule does not rigorously apply to the Si–C₂H₄ system, while we exclude the cave site by TE calculation easily here.

In order to study the influence of the broken dimer bond in our model, the Si₂₉H₃₀–C₂H₄ cluster with six more H atoms to saturate the broken dimer bond is adopted to calculate the binding energies on the four chemisorption sites mentioned above. The results show that the binding energy on the cave site is 0.11 eV less than that for the Si₂₉H₂₄–C₂H₄ cluster, and the influences on the other sites are even less than on the cave site. *It seems that the H*
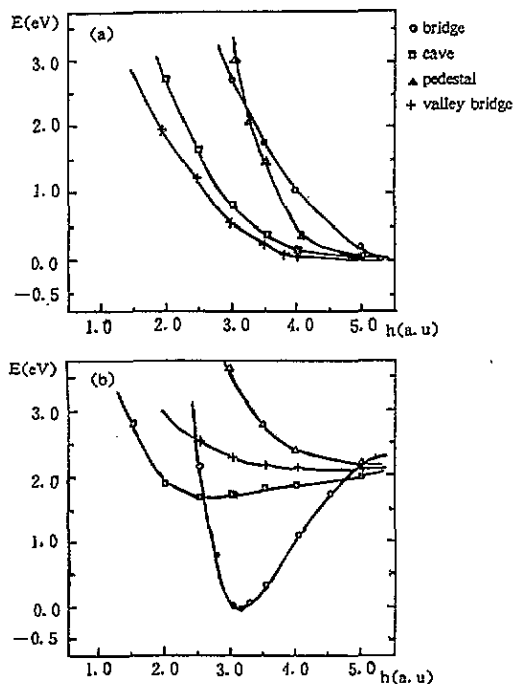
Figure 2. Curves of TE E versus the adsorption height h for ethylene adsorption on bridge (O), cave ($\square$), pedestal ($\triangle$) and valley bridge sites for (*a*) planar C_2H_4 adsorption and (*b*) rehybridized $C_2H_4^*$ adsorption: au, atomic units.

atoms to be used to saturate the broken dimer bonds have rather a small influence on our calculation, so we shall still use the $Si_{29}H_{24}$ cluster in further calculations below.

The two special cases above have given us much useful and direct information about the chemisorption geometry, but, as mentioned before, they are simple and incomplete. In order to obtain better understanding of the bonding structure, we must consider the TE variations with the C–C and C–H bond lengths, CH_2 scissors angle and CH_2 plane to the surface angle, etc. A method is employed in which one variable (e.g. the C–C bond length) is charged first while the others are fixed until an optimum is reached, next another variable is charged (the first variable, e.g. C–C bond length, is now set at the optimized value), and then the process is repeated again and again until the final results are convergent. Detailed calculations show that the bondings of C_2H_4 on the cave, pedestal and valley bridge sites are impossible. This is reasonable because of the poor overlap of C_2H_4 orbitals with surface dangling bonds on these sites. Thus, the only possible site is the bridge site, i.e. the dimer site.

Figures 3(*a*), 3(*b*) and 3(*c*) show the three intermediate TE variations for this optimization process for C_2H_4(ads) on the dimer site, namely the TE versus the C–C bond length d_{C-C}, the TE versus the CH_2 scissors angle θ_1, and the TE versus the angle θ_2 of the CH_2 plane to surface respectively. The variation in TE with C–H bond length is so
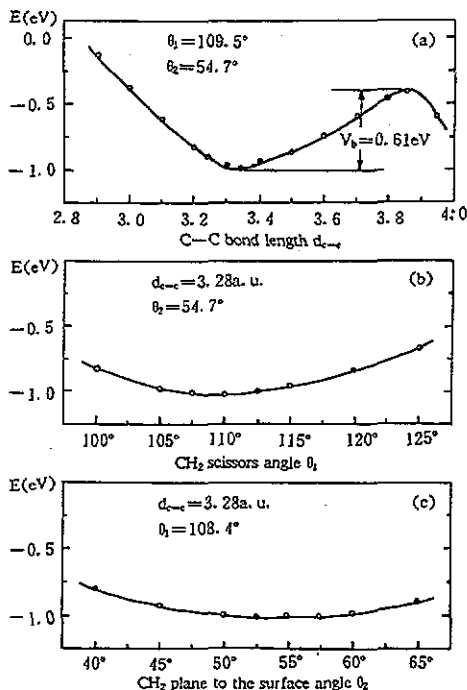
Figure 3. Curves of TE versus (*a*) the C–C bond length d_{C-C}, (*b*) CH$_2$ scissors angle θ_1 and (*c*) the angle θ_2 of the CH$_2$ plane to the surface.

small that we omit variation curve. Furthermore, we find that the convergence process is very fast. Hence, this method may be reliable and fast for multi-dimensional TE surface calculations.

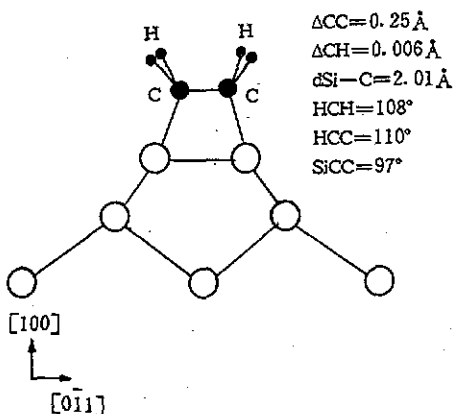**Figure 4.** Adsorption geometry for the di-σ-bonded C$_2$H$_4$ on dimer sites.

The final equilibrium di-σ-bonding geometry is shown in figure 4. The C–C bond length stretches 0.25 Å to a value near the single-bond value, indicating drastic weakening

of the C=C double bond (later vibrational frequency calculation also confirms this). The C–H bond length stretches only 0.006 Å, and the CH stretching frequency decreases about 2% (discussed later), which means the C–H bond is almost not weakened. This is similar to the very recent result obtained by Weiner *et al* [8] in their study of C_2H_2 on Si(111) using the Zener intermediate neglect of differential overlap theory, and the result obtained by our former study for C_2H_2–Si(111) using ASED theory [10]. Both the studies have revealed that the C–H bond of C_2H_2(ads) on Si(100) [10] and Si(111) [8] is only slightly weakened. (For comparison, the CH bond length stretches 0.02 Å and the CH stretching frequency decreases by about 11% for C_2H_2(ads) on Si(100).) The angles H–C–H, H–C–C, Si–C–C are near 108°, 110° and 97° respectively, i.e. a CH_2 scissors angle 108° and the CH_2 plane bends away 55° from the surface, indicating approximate sp^3 hybridization state for C atoms. The Si–C bond length is predicted to be 2.01 Å, a little larger than the bond length of 1.89 Å for the β–SiC crystal [28]. Overall, this di-σ-bonding geometry reveals that ethylene is rehybridized to an approximate sp^3 state to saturate the dangling bonds of two adjacent surface Si atoms. Then, why is ethylene distorted or rehybridized on Si(100)? As we know, the free molecule is unambiguously hybridized in the sp^2 state, i.e. in a planar structure (ASED theory has shown that the free-molecule distortion energy is 2.2 eV, as seen in figure 2). A reasonable explanation may be obtained by analysing the energy levels of free and distorted C_2H_4, and their behaviour when C_2H_4 adsorbs onto the Si(100) surface. Figure 5 shows the ground-state energy levels of free C_2H_4, distorted $C_2H_4^*$, substrate $Si_{29}H_{24}$ and the adsorbed systems C_2H_4/Si and $C_2H_4^*$/Si (on the dimer site). It is clear that, for the planar C_2H_2(ads), ethylene has only π donations to the surface because the antibonding π^* orbital is high above the Si surface orbitals. It is difficult for substrate dangling bonds to back-donate electrons to the empty π^* orbital. The resulting C_2H_4(ads) charge is +0.45 e, consistent with the π donation model. Although this π donation will result in some stability, it is not strong enough to cancel the repulsive interaction acting on C and H atoms from the substrate. This is why planar C_2H_4 cannot adsorb onto the Si(100) surface, whereas the situation for distorted $C_2H_4^*$(ads) is very different. The distortion causes the energy level of the π^* orbital to decrease by about 1.1 eV, i.e. it is 1.1 eV closer to the surface bands. Then it can be strongly back-donated by the Si surface radicals. So, for the rehybridized $C_2H_4^*$(ads), both π donation and π^* back-donation occur, which result in the equilibrium di-σ-bonding structure. The resulting C_2H_4(ads) charge of -0.30 e also confirms this donation and the back-donation process.

In order to confirm further the di-σ-bonding geometry, we calculated the vibrational frequencies of the C–C, C–H, and Si–C stretching modes and the CH_2 bending (scissoring, wagging, rocking and twisting) modes to compare with those found in the recent HREELS study. We used a Morse-type expression to simulate the curve of the TE versus the adsorption height or bond length near the equilibrium positions [29]:

$$E(x) = E_0 + \left[a + b(x - x_0) + c(x - x_0)^2\right]\left\{1 - \exp\left[-\alpha(x - x_0)\right]\right\}^2$$

where $E(x)$ is the TE at position x, x is the adsorption height or bond length, and x_0, E_0, a, b, c and α are the parameters to be found. Using this expression, we can obtain the equilibrium position x_0, the minimum TE E_0 and the force constants $k = (d^2E/dx^2)|_{x=x_0} = 2a\alpha^2$. A series of calculations have shown that this Morse-type expression can give more accurate force constants than the usual simple treatment using $E(x) = E_0 + b(x - x_0) + c(x - x_0)^2$.

Table 2 lists the calculated and observed vibrational frequencies for free gas and adsorbed ethylene on the dimer site. As mentioned in section 1, the theoretical frequencies for free gas are in good agreement with the experimental values [27]. For C_2H_4(ads) on the dimer
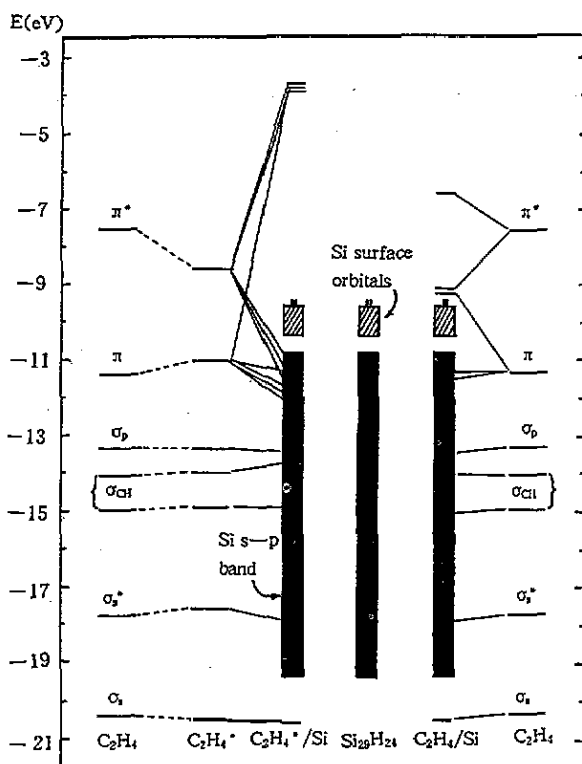
Figure 5. Ground-state energy levels of free C_2H_4, distorted $C_2H_4^*$, substrate $Si_{29}H_{24}$ and adsorbed systems C_2H_4/Si and $C_2H_4^*/Si$ for C_2H_4 adsorption on the dimer site.

Table 2. Calculated vibrational energies of C_2H_4- and C_2H_4-induced species on Si(100) 2×1. The vibrational energies for gas [27] and recent HREELS results [2] are included for comparison.

Mode	Free C_2H_4		Adsorbed C_2H_4	
	Theoretical	Experimental	Theoretical	Experimental
CH stretching	3011	3019	2952	2955
CC stretching	1504	1623	1030	1100
CH_2 scissors	1330	1342	1395	1440
CH_2 wagging	1163	949	1080	1260
SiC stretching			650	670
SiH stretching			2124	$\simeq 2120$
SiC stretching (C atom)			773	800

site, the CH stretching frequency decreases from 3011 to 2952 cm^{-1}, consistent with the HREELS result from 3019 to 2955 cm^{-1}. This small decrease (about 2%) in the CH stretching energy indicates that the CH bond is almost not weakened. For the CH_2 bending modes we selected only the scissoring and wagging modes for calculation. The CH_2 scissors and wagging frequencies are determined to be about 1395 cm^{-1} and 1080 cm^{-1}, respectively, in agreement with the HREELS results of 1440 cm^{-1} and 1260 cm^{-1}, respectively. The C–C stretching energy is predicted to be 1030 cm^{-1}, about 32% decrease from the gaseous value, which is also consistent with the experimental decrease of 32%. In other words, our calculated vibrational frequencies confirm the suggestion of the HREELS study for the

bonding geometry [2].

The frequencies of C(ads) and H(ads) (from the decomposition of C_2H_4(ads) on Si(100) are also included in table 2 (the bonding structures will be discussed later). They are in excellent agreement with the experimental values, which confirms again the validity of this simple method for vibrational frequency calculation.

Since the decomposition of the C_2H_4, C_2H_2, etc, small hydrocarbons on Si(100) can make it possible to grow high-quality single-crystal β-SiC films [5, 6, 8], we have studied the decomposition process of C_2H_4 on Si(100), and a preferential decomposition path of C_2H_4(ads) $\rightarrow$ CH_2(ads) $\rightarrow$ C(ads) + H(ads) $\rightarrow$ β-SiC is proposed.

To our knowledge, acetylene on Si(100) favours the decomposition path C_2H_2(ads) $\rightarrow$ C_2(ads) + H(ads) $\rightarrow$ C(ads) $\rightarrow$ β-SiC [1, 10]. The activation barrier for C_2H_2(ads) $\rightarrow$ CH(ads) + CH(ads) is estimated to be 2.2 eV, much larger than that for C_2H_2(ads $\rightarrow$ C_2H(ads) + H(ads) (about 0.80 eV). This means that C_2H_2(ads) undergoes dehydrogenation first and then C–C bond scission [10], while the state for C_2H_4(ads) on Si(100) is somewhat different. The C–C bond scission (i.e. C_2H_4(ads) $\rightarrow$ CH_2(ads) + CH_2(ads), shown in figure 3(a)) is only endothermic by about 0.6 eV, while the dissociation of one H atom from C_2H_4(ads) must overcome an activation barrier of about 0.9 eV (estimated on the basis of the transition of one H atom away from C_2H_4(ads)). That is to say, ethylene favours C–C bond scission over dehydrogenation. The different decomposition path of C_2H_4(ads) and C_2H_2(ads) on Si(100) may be explained by analysing the C–C bond orders. The C–C bond order of C_2H_2(ads) on Si(100) is still greater than unity although it is weakened by the surface dangling bonds. It is more difficult to scissor the C–C bond than to break the C–H bonds. For C_2H_4(ads) its C–C bond is weakened to a nearly single nature, and it is easier to break than the C–H bonds. This has been confirmed by the HREELS results [2], which have shown that C_2H_4 is adsorbed non-dissociatively at 77–600 K and, by heating to 650 K, some of the ethylene is desorbed while the rest is decomposed to CH_x ($x = 1, 2$). In contrast, some of the C_2H_2(ads) on Si(100) is desorbed while the rest is decomposed to C_2H_x ($x = 0, 1$) by heating to 750 K).

Certainly, ethylene decomposition on Si(100) is also very different from that on transition metals. On Fe(100) [12], Ni(111) [13] and Mo(100) [13], C_2H_4(ads) is dehydrogenated to form C_2H_2(ads) at 310 K, 230 K and 220 K, respectively. On Pd(100) [15] and Ni(100) [15], C_2H_4(ads) is dehydrogenated to form $CHCH_2$ (vinyl) at 250 K and 200 K, respectively. On Pt(111)([17], ethylene is dehydrogenated to form CCH_3 (ethylidene) at 220 K. Ethylene adsorbed on Ru(0001) is dehydrogenated to form CCH_3 and CCH (ethynyl) at 150 K. Moreover, our group's recent ASED study of the dehydrogenation of C_2H_4 and C_2H_2 on Mo(100) has found no significant activation barriers. Similar results have also been obtained by Kang and Anderson [19] in their ASED study of C_2H_4 and C_2H_2 adsorption on Pt(111) [19]. In summary, ethylene on transition metals will produce more intermediates than on Si surfaces, and in most cases the decomposition on transition metals is much easier.

Finally, the bonding geometries of dissociated C and H atoms are discussed. Both C and H atoms adsorb onto the surface dangling bonds. The Si–C bond length is optimized to be 1.75 Å, 0.26 Å less than that for the adsorbed C_2H_4 molecule (2.01 Å) and is very close to the diatomic SiC bond length of 1.70 Å [30]. The angle of the Si–C bond to the surface normal is nearly 19°, and the binding energy is 2.17 eV. The Si–H bond is very similar to the Si–C bond, but with a bond length of 1.56 Å and a binding energy of 1.65 eV. The Si–C and Si–H stretching frequencies are calculated to be 773 cm^{-1} and 2124 cm^{-1}, respectively, in excellent agreement with the observed values of 800 cm^{-1} and about 2120 cm^{-1} [2].

4. Conclusions

The adsorption and decomposition of ethylene on the Si(100) 2×1 surface, as well as the vibrational properties have been studied by ASED molecular orbital theory. A summary of the important results are as follows.

(i) Ethylene is di-σ bonded to the surface dimer sites with a rehybridization state approximately sp^3. The C=C double bond is transformed to a nearly single bond, while the C–H bonds are almost not weakened. The C–C and C–H bond lengths stretch 0.25 Å and 0.006 Å, respectively. The Si–C bond length is predicted to be 2.01 Å.

(ii) In the adsorption process, the planar C_2H_4 has only π donations to the surface, while the distorted $C_2H_4^*$ has both π donations and π^* back-donations from surface radicals, which result in the equilibrium di-σ bonding geometry.

(iii) The decomposition of C_2H_4 on Si(100) is somewhat different from that for C_2H_2(ads) on Si(100) and from C_2H_4(ads) on transition metals. Ethylene favours C–C bond scission first and then dehydrogenation. The activation barrier of the C–C bond scission is estimated to be about 0.6 eV, while the dissociation of one H atom from C_2H_4(ads) is found to be endothermic by about 0.9 eV.

(iv) The vibrational properties are calculated in detail. Most of the results are in good agreement with the observed values, which confirm the suggestion of di-σ-bonding geometry obtained from the HREELS study.

References

[1] Nishijima M, Yoshinobu J, Tsuda H and Onchi M 1987 *Surf. Sci.* **192** 383
[2] Yoshinobu J, Tsuda H, Onchi M and Nishijima M 1987 *J. Chem. Phys.* **87** 7332
[3] Yoshinobu J, Tsuda H, Onchi M and Nishijima M 1986 *Chem. Phys. Lett.* **30** 170
[4] Yoshinobu J, Tsuda H, Onchi M and Nishijima M 1986 *Solid State Commun.* **60** 801
[5] Cheng C C, Wallace R M, Taylor P A, Choyke W J and Yates Jr J T 1990 *J. Appl. Phys.* **67** 3693
[6] Cheng C C, Choyke W J and Yates Jr J T 1990 *Surf. Sci.* **231** 289
[7] Chu S Y and Anderson A B 1988 *Surf. Sci.* **194** 55
[8] Weiner B, Carmer C S and Frenklach M 1991 *Phys. Rev.* B **43** 1678
[9] Bozack M J, Taylor P A, Choyke W J and Yates Jr J T 1986 *Surf. Sci.* **177** L933
[10] Zhou Ru-Hong, Cao Pei-Lin and Lee Lie-Quan 1993 *Phys. Rev.* B **47** at press
[11] Albent M R and Yates Jr J T 1987 *The Surface Scientists Guide to Organometallic Chemistry* (Washington, DC: American Chemical Society)
[12] Erley W, Baro A M and Ibach H 1982 *Surf. Sci.* **120** 273
[13] Lehwald S and Ibach H 1979 *Surf. Sci.* **89** 425
[14] Wang L and Tysoe W T 1990 *Surf. Sci.* **236** 325
[15] Stave E M and Madix R J 1985 *J. Phys. Chem.* **89** 105
[16] Zaera F and Hall R B 1987 *Surf. Sci.* **180** 1
[17] Steininger H, Ibach H and Lehwald S 1982 *Surf. Sci.* **117** 685
[18] Hills M M, Parmeter J E, Mullius C B and Weinberg W H 1986 *J. Am. Chem. Soc.* **108** 3554
[19] Kang D B and Anderson A B 1985 *Surf. Sci.* **155** 639
[20] Roberts N and Needs R J 1990 *Surf. Sci.* **236** 112
[21] Domanek D and Bennemann K H 1985 *Phys. Rev.* B **31** 2485

[22] Cao Pei-Lin and Zhang Zhong-Guo 1989 *Phys. Rev.* B 39 9963
[23] Zhou Ru-Hong, Shi Dai-Hua and Cao Pei-Lin 1992 *J. Phys.: Condens. Matter* 4 2429
[24] Cao Pei-Lin, Zhou Ru-Hong and Zhou Xu-Yan 1979 *Phys. Lett.* 159A 179
[25] Lotz W 1970 *J. Opt. Soc. Am.* 60 206
[26] Clementi E and Raimondi D L 1963 *J. Chem. Phys.* 38 2686
[27] Hertzberg G 1945 *Molecular Spectra and Molecular Structure* vol II *Infrared and Raman Spectra of Polyatomic Molecules* (New York: Van Norstrand)
[28] Donnay J D H and Ondik H M 1973 *Crystal Data, Determinative Tables* vol II *Inorganic compounds* 3rd edn (Washington, DC: US Department of Commerce)
[29] Zhou Ru-Hong and Cao Pei-Lin 1993 *Surf. Sci.* accepted
[30] Huber K D and Hertzberg G 1979 *Molecular Spectra and Molecular Structure* vol IV *Constants of Diatomic Molecules* (New York: Van Norstrand)